BIODIVERSITAS
Volume 24, Number 12, December 2023
Pages: 6502-6515

ISSN: 1412-033X
E-ISSN: 2085-4722
DOI: 10.13057/biodiv/d241212

Antimicrobial and FAD synthetases modulating activities of leporins A-C isolated from the sponge-associated fungus *Trichoderma* sp.

FITJE LOSUNG[1], ELVY L. GINTING[1], BOBBY ABDJUL[2], MAGIE M. KAPOJOS[3], WILMAR MAARISIT[4], FENY MENTANG[1], DEISKE A. SUMILAT[1], WALTER BALANSA[1,5,♥], REMY E. P. MANGINDAAN[1,♥♥]

[1]Faculty of Fisheries and Marine Science, Universitas Sam Ratulangi. Jl. Kampus-Bahu, Manado 95115, North Sulawesi, Indonesia. Tel.: +62-431-868027, ♥♥email: remymangindaan@unsrat.ac.id
[2]North Sulawesi Research dan Development Agency. Jl. 17 Agustus Manado-95000, North Sulawesi, Indonesia
[3]Faculty of Science and Technology, Universitas Prisma. Jl. Pumorow, Tikala, Manado 95000, North Sulawesi, Indonesia
[4]Department of Pharmacy, Faculty of Mathematics and Natural Sciences, Universitas Kristen Indonesia Tomohon. Jl. Raya Talete II, Kuranga, Tomohon 95441, North Sulawesi, Indonesia
[5]Department of Fisheries and Maritime Technology, Polikteknik Negeri Nusa Utara. Jl. Kesehatan 1 Tahuna, Sangihe, North Sulawesi, Indonesia. Tel.: +62-432-24745, ♥email: walterbalansa1@gmail.com

Manuscript received: 16 August 2023. Revision accepted: 17 December 2023.

Abstract. *Losung F, Ginting EL, Abdjul B, Kapojos MM, Maarisit W, Mentang F, Sumilat DA, Balansa W, Mangindaan REP. 2023. Antimicrobial and FAD synthetases modulating activities of leporins A-C isolated from the sponge-associated fungus* Trichoderma *sp. Biodiversitas 24: 6502-6515.* The emergence of microbial resistance poses a formidable threat to human health, requiring the discovery of new antibiotics. In this study, we investigated the antimicrobial potential and molecular structures of the metabolites produced by a sponge's symbiont fungal species, *Trichoderma* sp., *in vitro* against *S. aureus* IAM 12544T and *Candida albicans* IFM 4954 and in-silico against the emerging antibacterial target, prokaryotic bifunctional synthetases (FADS). The molecular structures were determined using spectroscopic techniques (1D, 2D NMR, HRESIMS), while the assessment of biological activities, physicochemical properties, and molecular modifications was performed through a slightly modified disk agar diffusion method, molecular docking, SwissAdme and pkCMS tools, and bioisosterism, respectively. The analysis of spectroscopic data supported the identification of leporins A-C (**1-3**) as the metabolites, which exhibited strong binding affinities against the 2X0K protein target (–8.9 to –9.4 kcal/mol). Despite their being slightly weaker than known FADS modulators such as compounds **4** (–10.5 kcal/mol) and **5** (–10.5 kcal/mol), leporins A-C demonstrated a stronger binding affinity than compound **6** (–9.6 to –10.5 kcal/mol). Notably, substituting a methyl group with a fluorine atom in **1-3** resulted in lepofluorins A-C (**1a-3a**), which exhibited enhanced binding affinities and improved physicochemical properties compared to the existing FADS modulators. These findings suggest that leporins A-C (**1-3**), particularly lepofluorins A-C (**1a-3a**), have potential as putative novel modulators of FADS. This study provides valuable insights into the design and development of new antibiotics to combat microbial resistance.

Keywords: Antibacterial, bioisosterism, in-silico, pyridine, *Trichoderma* sp.

Abbreviations: FMN: Favin Mononucleotide, FAD: Flavine Adenine Dinucleotide

INTRODUCTION

Infectious diseases remain a profound and global health concern for humanity, posing a substantial threat to public health (Iscla et al. 2015; Dinghra et al. 2020; Tondi 2021; Pariente et al. 2022). Despite their debatability (de Kraker et al. 2016), they are expected to cause an estimated 10 million deaths annually by 2050 (O'Neil 2014). However, while bacterial infections are on the rise, the advancement of new antibiotic discoveries in both preclinical and clinical stages has stagnated (WHO 2021; Tondi 2021). According to The World Health Organization (WHO), only twelve antibiotics have received FDA approval since 2017, notably ten belonging to known classes featuring recognized mechanisms of antimicrobial resistance. One possible explanation for this trend is that the majority of new antibiotic candidates are derivatives of existing antibiotics (Iscla et al. 2015; Hutchings et al. 2016), resulting in shorter periods of efficacy against pathogenic bacteria compared to novel antibiotics (Coates et al. 2011). Collectively, these factors highlight the pressing demand for the discovery of new antibiotics (Theuretzbacher et al. 2015; Thakare et al. 2020), particularly those derived from natural sources, due to their molecular complexity, multiple microbial targets, and lower susceptibility to microbial resistance (Terenni et al. 2021).

Many natural products, especially microbial natural products, demonstrate significant chemical diversity and antibiotic efficacy, including but not limited to teixobactin (Ling et al. 2015). Armed with a unique scaffold, teixobactin kills bacteria through a two-pronged attack on the bacterial cell envelope (Shukla et al. 2022), therefore escaping the pre-existing resistance issue and suggesting a valid solution to fight microbial resistance (Ling et al. 2015). Additionally, while more than 90% of soil and marine microorganisms remain uncultivated (Ling et al. 2015; Indraningrat et al. 2016), the majority of clinically used antibiotics are derived from microorganisms or

microbial derivatives, underscoring the untapped potential of microbes, especially uncultivated microbes, as a major source of new antibiotics (Ling et al. 2015; Schneider et al. 2021). However, the antibiotics were mainly isolated from microbes cultivated using various culture-dependent techniques, which were considered tedious, time-consuming, and non-reproducible (Khabthani et al. 2021). Moreover, according to Schneider et al. (2021), bioprospecting microbial antibiotics is labor-intensive, expensive, and low yield, limiting the microbes' ability to serve as a major source of new antibiotics. Together, these factors highlight the limitations of traditional antibiotic discovery strategies and the need to complement them with emerging technologies such as computational studies to support new antibiotic discovery endeavors (Khabthani et al. 2021).

Indeed, the emergence of bioinformatics has resulted in a significant change across a wide range of academic disciplines, including antibiotic drug discovery (Farhat et al. 2023). The authors highlight the accelerated and efficient nature of the in-silico methodology, which is reshaping modern drug discovery, including antibiotic discovery. This method simplifies the identification of potential antibiotics through diverse approaches, one of which involves molecular docking to specific protein targets crucial for bacterial biosynthesis, such as prokaryotic bifunctional FAD synthetases (FADS) (Sebastian et al. 2018). Considering the pivotal role of FADS in synthesizing flavin mononucleotide (FMN) and flavin adenine dinucleotide (FAD) within bacterial contexts (Serrano et al. 2013), compounds modulating bacterial FADS hold promise as selective antimicrobial agents (Serrano et al. 2013; Sebastian et al. 2018). Nevertheless, while FAD modulators show potential as an emerging target in antibiotic discovery (Serrano et al. 2013; Sebastian et al. 2018) and *in silico* studies have demonstrated their efficiency in discovering new antibiotics (Iscla et al. 2015; Khabthani et al. 2021; Stokes et al. 2020), the search for new FAD modulators through computational studies, particularly leveraging marine resources, remains limited.

This study aimed to determine the molecular structures of the isolated metabolites from the sponge-associated fungus *Trichoderma* sp., to assess the *in vitro* antimicrobial activity of the metabolites against the Gram-positive *S. aureus* IAM 12544T and the fungus *Candida albicans* IFM 4954 and to conduct molecular docking as well as ADMETox analysis of these metabolites against the specific target protein (2X0K) associated with the FAD enzyme. This study sheds new light on the antibacterial potential of *Trichoderma* sp. metabolites as potential new modulators of the FADS enzyme by combining *in vitro* and *in silico* approaches.

MATERIALS AND METHODS

Study area

The sponge from which the fungus *Trichoderma* sp. isolated was collected from Malalayang Beach in Manado Bay, North Sulawesi, Indonesia, as indicated by a red dot on the map.

Procedures

Sample collection

The sponge was collected by hand using SCUBA diving in the coastal waters of Malalayang at a depth between 5 and 10 m, about 100 m from the shoreline, in July 2015 (Figure 1). The seawater salinity was 30 ppt, and the temperature was 25-28°C during the specimen collection.

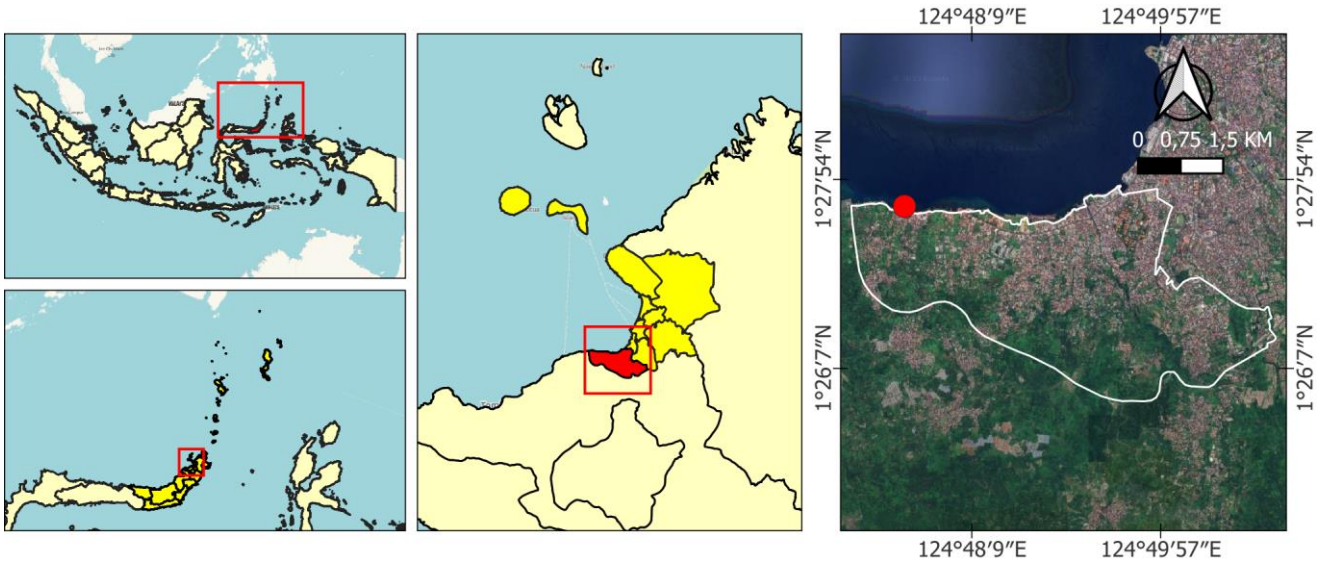

Figure 1. Location of Malalayang Beach Manado Bay (red dot), indicating the sampling sites of the sponge *Stelletta clavosa* (01º27'39'' N dan 124º47'31''E), Manado, North Sulawesi, Indonesia (Google Maps 2023)

Fungal identification

The fungus was isolated from a marine sponge, *Stelletta clavosa*, collected between 5 and 10 m deep in Malalayang Beach, Manado Bay, Indonesia, at a geographical position of 01º27'39" N and 124º47'31" E. A small portion of the sponge (~1 cm) was taken, washed twice in 2 mL of sterilized 50% seawater containing 200 µg/mL chloramphenicol, and dipped in a sterilized plate for four hours containing the same solution. Each piece was then inoculated onto a yeast-soluble agar (YSA) plate and incubated for three days at room temperature. Harvested mycelia were cultivated on an agar plate (glucose 2%, polypeptone 1%, yeast extract 0.5%, chloramphenicol 200 µg/mL, and agar 2% in 90% seawater). Only taxonomically identified fungal colonies would be subjected to further chemical investigation. The fungus was inoculated into flasks containing rice medium and incubated for two weeks at room temperature. Only Total fungal DNA extraction was conducted using the Innu Prep DNA Micro Kit (Analityk Jena, Germany). ITS1 (5′-TCC GTA GGT GAA CCT GCG-3′) and ITS4 (5′-TCC TCC GCT TAT TGA TAT GC-3′) primers were used to amplify the nuclear ribosomal internal transcribed spacer (ITS) region using Polymerase Chain Reaction (PCR) MyTaq™ HS Red Mix (Bioline) according to White et al. (1990). Reaction condition for PCR using two primers: denaturation at 94°C (five minutes), followed by 35 denaturation cycles at 95°C (30 seconds), annealing at 52°C (30 seconds), and extension at 72°C (30 seconds). Every reaction (40 µL) contained 15 pmol of each primer and DNA template. Reaction composition: 20 µL MyTaq HS Red Mix, 1.5 µL each primer (10 µM), 15 µL ddH2O, and 2 µL DNA template. The PCR results were separated using electrophoresis gel agarose 0,8% (in TBE buffer 1x) and electrified for 30 minutes at 100 V. It was observed using a UV-transilluminator after being stained with ethidium bromide for 10 minutes. PCR's success was marked by the presence of a single band (600 bp). The PCR results and both primers were sent to First Base CO (Malaysia) for sequencing. The obtained DNA sequences were modified and compared using the ClustaW algorithm (Thompson et al. 1994). Identification was done using GenBank (www.ncbi.nlm.nih.gov). The phylogenetic tree was constructed using the software Geneious v5.6 and the Neighbor-Joining algorithm.

Fungal isolation and extraction

Four fungal isolates (FL541, FL542, FL543 and FL544) from the sponge *Stelletta clavosa* were isolated using the 'Bathing' method (Kobayashi et al. 2006). Briefly, sterile seawater (50%) with 200 µg/mL chloramphenicol was used to wash sponge pieces, followed by a 24-hour soak. The sponge pieces were then placed on Yeast Extract Agar (YSA, DIFCO) with antibiotics and incubated. Fungi around the sponge pieces were observed, separated, and recultivated on antibiotic-free media. Different fungal pure colony were separately inoculated on sterile rice media and cultured for two weeks. All cultivated fungi were harvested and individually underwent maceration with ethyl acetate (EtOAc), and their EtOAc crude extracts, obtained after filtration and evaporation, were tested against *S. aureus* and *C. albicans* FH2173. Only isolates whose extracts showed strong antimicrobial activity (isolate FL541) underwent further detailed chromatographic and spectroscopic analyses.

Antimicrobial assay

The anti-microbial activity of fungal crude extract was tested using the agar diffusion method (Kirby-Bauer). In brief, to the sterilized Mueller Hinton Agar (DIFCO) medium was added 1.0 mL of the test bacteria *E. coli* ATCC35218 and *S. aureus* ATCC33592 with a density of 103 CFU/mL. After the medium was dry, a paper disc (diameter 6 mm) was placed on it, then dripped with 50 µL of the test extract and incubated at room temperature for 24 hours. The antibiotic chloramphenicol and ketoconazole (100 µg/mL) (Kimia Farma) were used as positive controls, while the ethyl acetate (EtOAc) solvent was used a negative control. Following the incubation, inhibition zone was observed, diameter was measured and compared to the controls.

Isolation of compounds 1-3

The fungal EtOAc extract was evaporated under reduced pressure, and the residue (1.2 g) was fractionated by an ODS column (100 g). The column was eluted stepwise with each 500 mL of MeOH in H_2O (30, 50, 70, 85, and 100%). The fractions (1-5) were collected and analyzed. The active fraction 4 (85% MeOH eluate, 85.3 mg) was purified in an isocratic mode using an HPLC column (Pegasil ODS, Senshu Sci. Co. Ltd., Tokyo, Japan), 10 × 250 mm; 76% MeOH solvent; flow rate, 2.0 mL/min; and UV detection at 210 nm. Preparative HPLC was carried out using the L-6200 system (Hitachi Ltd., Tokyo, Japan). PerkinElmer Spectrum One Fourier transform infrared spectrometer (Waltham, MA, USA) was used to measure the IR spectra. EI mass spectra were obtained from a JMS-MS 700 mass spectrometer (JEOL, Tokyo, Japan). NMR spectra of 1H and ^{13}C were recorded on a JNM-AL-400 NMR spectrometer (JEOL) at 400 MHz for ^{1}H and 100 MHz for ^{13}C in CD3OD (δH 3.30, δC 49.0).

Structure determination of leporins A and B

Leporin A (3): Yellow oils; EIMS m/z 365 $[M]^+$; ^{1}H NMR (CD_3OD) δ 7.71 (s, ^{1}H, H-3), 7.29-7.42 (m, 5H, H-18, H-19, H-20, H-21, H-22) 5.82 (dq, *J*=16.0, 8.0 ^{1}H, H-15), 5.39 (dd, J=16.0, 8.0, ^{1}H, H-14), 4.93 (m, ^{1}H, H-13), 4.00 (s, 3H, H-23), 2.76 (dd, J=12.0, 4.0, 1H, H-7), 1.76 (m, ^{1}H, H-12), 1.72 (dd, *J*=8.0, 4.0, 3H, H-16), 1.63 (m, ^{1}H, H-8), 1.01-1.83 (m, 6H, H-9, H-10, H-11), 0.95 (d, *J* =6.0, 3H, H-23) ; ^{13}C NMR (CD_3OD) δ 160.4 (C-1), 158.3 (C-5), 135.7 (C-17), 133.3 (C-3), 132.5 (C-15), 130.7 (C-14), 130.4 (C-18, C-22), 129.1 (C-19, C-21), 128.5 (C-20), 113.7 (C-4), 111.8 (C-6), 79.5 (C-13), 65.5 (C-24), 39.3 (C-7), 37.2 (C-8, C-12), 36.5 (C-9), 27.6 (C-11), 21.8 (C-10), 21.1 (C-23), 17.9 (C-16).

Leporin B (2) : Yellow oils; EIMS *m/z* 351 $[M]^+$; 1H NMR (CD_3OD) δ 7.63 (s, ^{1}H, H-3), 7.28-7.42 (m, 5H, H-18, H-19, H-20, H-21, H-22), 5.81 (dq, *J*=14.0, 8,0, 1H, H-15), 5.40 (dd, J=14.0, 8.0, ^{1}H, H-14), 4.90 (m, ^{1}H, H-13),

2.77 (br d, *J*=12,0 1H, H-7), 1.76 (m, ^{1}H, H-12), 1.72 (br d, *J*=8.0, 3H, H-16), 1.60 (m, ^{1}H, H-8), 1.28-1.79 (m, 6H, H-9, H-10, H-11), 0.95 (d, *J* =8.0, 3H, H-23) ; ^{13}C NMR (CD_3OD) δ 160.4 (C-1), 158.3 (C-5), 135.7 (C-17), 133.3 (C-3), 132.5 (C-15), 130.7 (C-14), 130.4 (C-18, C-22), 129.1 (C-19, C-21), 128.5 (C-20), 113.7 (C-4), 111.8 (C-6), 79.5 (C-13), 65.5 (C-24), 39.3 (C-7), 37.2 (C-8, C-12), 36.5 (C-9), 27.6 (C-11), 21.8 (C-10), 21.1 (C-23), 17.9 (C-16).

Leporin C (1): Yellow oils; [α]22D -17.6 (c 0.10, MeOH); IR (KBr) v_{max} 3431, 2927, 2864, 1642, 1452, 1428, 1217,965 cm-1; ^{1}H and ^{13}C NMR (CD_3OD), see Table 1; EIMS *m/z* = 335 $[M]^+$; HREIMS m/z 335.1885 $[M]^+$, Δ 0.0 mmu.

Docking studies

Target protein preparation. The docking of all ligands (leporin A and B) and FDA-approved drugs (anastrozole, citacapebin, and epirubicin) inside the protein targets (2X0K) was performed using CB-Dock 2 (Liu et al. 2022). The pdb files for the crystal structures of the protein target (PDB ID: 2X0K: resolution 3.01 Å) was retrieved from the protein databank website (http://www.rcsb.org/pdb).

Ligand preparation. The 2D structures of all ligands were drawn using ChemiDraw Ultra 12.0. The cdx files of the 2D structures were uploaded, optimized (MM2), converted to, and saved in Mol2 file format by Chem3D Pro 12 before using them in molecular docking.

Molecular docking. Molecular docking was performed using the CB-Dock2 server (http://cadd.labshare.cn/cb-dock2/index.php), adopting a blind approach (Liu et al. 2022). According to the authors, CB-Dock2 achieved an 85.9% success rate within the top-ranking pose of 2.0 Å root mean squared deviation (RMSD) compared with the crystal structure. In addition, it exceeded 69.4% of CB-Dock or 83.5% of FitDock significantly, and when compared to other state-of-the-art blind docking servers, such as MtiAutoDock, SwissDock, and COACH-D, CB-Dock2 was claimed to exhibit a 16% higher success rate (Liu et al. 2022).

ADMET assessment. The isomeric SMILES of all molecular structures of the FADS modulators were retrieved from PubChem for the small molecules available in the database and from 3D Chem for the remaining ligands. The SMILES were uploaded to the ADMET property analysis online tool at http://www.swissadme.ch/website (Daina et al. 2016).

RESULTS AND DISCUSSION

Sponge symbiotic microorganisms have been recognized as a good source of antimicrobial agents for many years (Indraningrat et al. 2016). According to the authors, bacteria were the most abundant sponge symbiont, accounting for 35 genera of bacteria compared to 12 genera of fungi, with the latter accounting only for 34% of all known sponge symbionts. The data suggest the rarity of metabolites in sponge-associated fungi, as well as their relatively unexplored potential compared to sponge-symbiotic bacteria. Furthermore, studies have frequently reported leporins A-C (**1**-**3**) as the major metabolites of terrestrial fungi such as *Aspergillus* with insecticidal, antimicrobial, anticancer, and antidiabetic type-2 activities (TePaske et al. 1991; Tao et al. 2017; Okamoto 2022). However, the present study describes for the first time leporins A-C from sponge-associated fungi of the genus *Trichoderma*. Although a fungus belonging to the same genus has been reported as a sponge symbiont (Setyowati et al. 2017), to date, leporins have never been reported from *Trichoderma* fungi. More importantly, we were the first to conduct an in-silico study to explore the antibacterial potential of leporin A-C against the emerging antibacterial target, FADS enzyme. Therefore, this study gives a new insight into marine sponge symbiotic fungi as a new source of leporin A-C as well as the antibacterial activity of the rare pyridone-containing compounds against the FADS enzyme, as follows:

Fungal identification

The molecular identification of fungal isolate code 4 has been achieved and resulted in a striking 100% genetic similarity to the *Trichoderma* fungus. This resemblance was visually confirmed through a phylogenetic tree (Figure 2).

Structure elucidation of leporins

Compound **1** was obtained as yellow oil. The HRESIMS of **1** showed a molecular ion at *m/z* 335.1885 $[M]^+$ (Figure 3A) corresponding to a molecular formula of $C_{22}H_{25}NO_2$ with 11 degrees of unsaturation. The ^{1}H (Table 1) and ^{13}C (Table 1) NMR spectra of compound **1** (in CD_3OD) revealed the presence of four major functional groups: mono-substituted benzene (δ_H 7.38, 7.34, 7.27, 7.34.7.38, δ_C 130.3, 129.1, 128.2, 129.1 and 130.3, 135.7), a pyridone (δ_H 7.18, δC 165.4, 132.6, 117.2, 162.2, 112.7 and 38.6), a fused dihydropyran (δ_H 1.76, 4.93; 37.2, 79.5, 38.6, 162.2, 112.7) and a cyclohexane ring (δ_H 1.61, 162, 1.23, 153, 1.28, 179, 1.61, 1.76; δc 38.6, 37.4, 36.5, 21.8, 27.6, 37.2) (Figure 3B). Together, they feature four rings and six double bonds, constructing 10 of the 11 degrees of unsaturation in **1**, indicating **1** as a tetracyclic molecule.

The presence of one aromatic and three non-aromatic rings in **1** was established by analyzing the 1D and 2D NMR data of **1** (Table 1) and comparing them to the reported values for the known leporin C as follows: A monosubstituted benzylic moiety was confirmed by two pairs of identical ortho and meta-coupled aryl protons at δ 7.38 (dd, *J* = 8.2, 1.4 Hz) (H-18, H-22) and at δ_H 7.34 (dd, *J* = 8.2, 7.2 Hz, H-19, H-21), one multiplet aryl proton at δ_H 7.23 (H-20), a benzylic carbon at δ 135.7 (C-17), and HMBC correlations for H-19/C-17, H-20/C18, H-21/C-17, H-18/C-4, H22-C-4 (Table 1), thus placing the aromatic group at C-4 of the pyridone moiety. The pyridone was supported by HMBC correlations between H-3 and C-1, C-4, and C-5. The existence of a dihydropyran was established by two methine protons at δ_H 2.71 (dd, 10.9, 3.6 Hz) and HMBC correlations between H-7 and C-5, C-6, C-7, and C-12. Moreover, contagious COSY correlations from H-7 to H-8 through H-12 and HMBC correlations between H-7 and C-8, C-5, C-6, C-9, and C-12 supported

the presence of a fused cyclohexyl and the dihydropyrans rings. The HMBC connections between H-23/C-7, C-8, and C-9 placed the methyl group at C-8 of the cyclohexyl moiety. Further, extensive COSY correlations from H-13 to H-14 through H-16 and HMBC correlations between H-13 and C-7, C-12, C-14, and C-15 positioned a propenyl moiety at C-13 of the dihydropyran functionality (HBMC and COSY correlations (Figure 4A). Finally, because of the large coupling constants of the vinyl protons at δ 5.40 (J = 15.2 Hz) and δ 5.82 (J = 15.2 Hz), the propenyl was assigned the *E* geometry and satisfied the 11 double bond equivalents in **1**. Collectively, they allowed the assignment of the planar structure of **1** as shown, matching that of leporin C (TasPaske 1991).

To determine whether compound **1** was a new derivative or the known compound leporin C, we investigated the relative stereochemistry of **1** by measuring and analyzing the NOESY spectrum in CD_3OD. NOE correlations between H-8 (δ_H 1.61)/H-13 (δ_H 4.93) and H-12 (δ 1.76)/H-14 (δ 5.40) revealed that compound **1's** relative configurations at position 7, 8, 12, and 13 were identical to those of leporin B (Zhang et al. 2013). This was reinforced further by the coupling constant between H-7/H-8 (J 7,8=10.9 Hz) and H-12/H13 (J 12,13=11.1 Hz). As a result, the structure of compound **1** was elucidated, as shown in Figure 2, featuring the exact structure of the known pyridone-containing molecule called leporin C, first reported as a synthetic intermediate product of (+/–)-leporin A (Snider and Lu 1996) and later as a natural product from the fungus *Scytalidium cuboideum* (Turner 2017).

Leporins A (2) and B (3)

Compounds **2** and **3** were also obtained as yellow oil. Their molecular formula was estimated as $C_{22}H_{25}NO_3$ and $C_{23}H_{27}NO_3$ based on their molecular ions at *m/z* 351 $[M+H]^+$ and 365 $[M+H]^+$ respectively and showed similar ^1H NMR and ^{13}C spectra to leporin C except for the presence of hydroxyl and methoxyl groups in **2** and **3** respectively. This was further supported by compounds **2** and **3** being 16 and 30 mass units heavier, compared to compound 1, indicating **2** and **3** as hydroxylated and methoxylated derivatives of compound **1** respectively (Figure 4B). The relative stereochemistry of **2** and **3** were tentatively assigned similarly to **1** because they were isolated from the same sample. Hence, the structures of leporins A-C were established as shown in Figure 3. Leporin C has been reported to exert various biological activities, including potent anti-insect activity against and moderate antibacterial activity (Turner 2017) and anti-viral Sar-Cov-2 (Forrestall et al. 2021). In addition, while leporin B was reported as an anticancer and anti-diabetic (Okamoto et al. 2022), leporin A was documented as a potent antibacterial against seven bacteria including MRSA (Tao et al. 2017). To date, there has been no single report on leporin A-C from sponge symbiotic fungus, nor has their antimicrobial potential against the FADS enzyme been investigated.

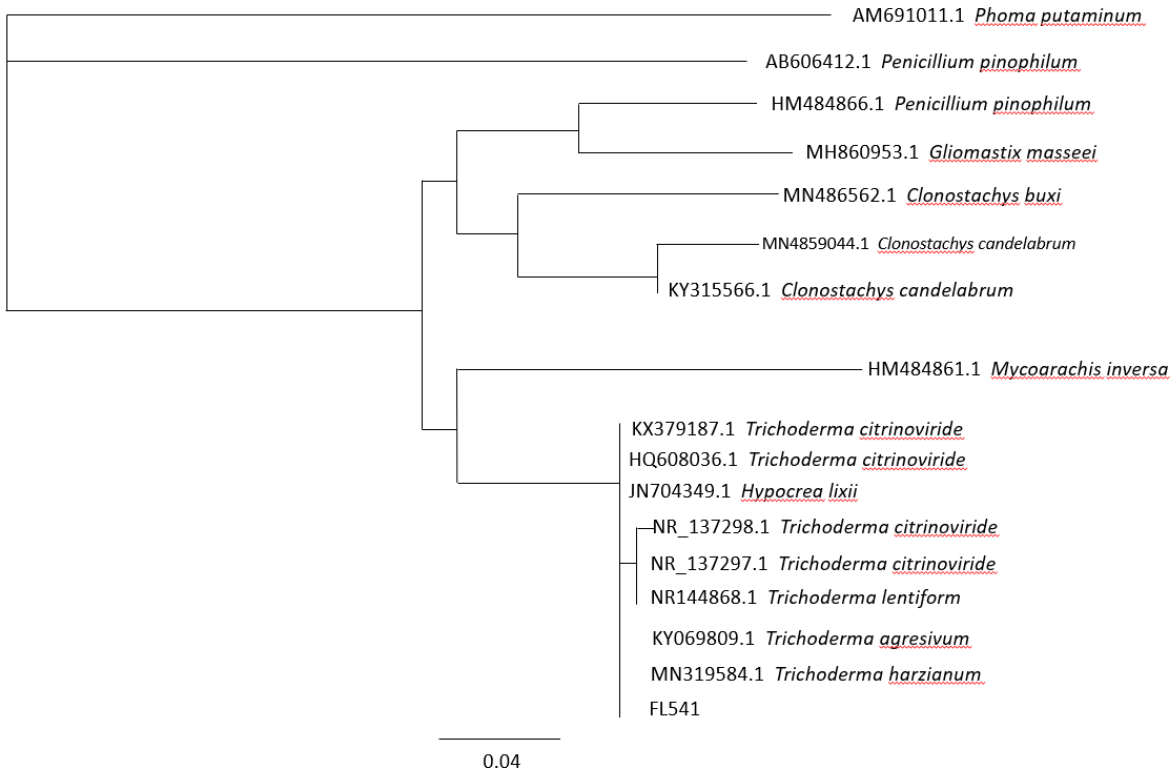

Figure 2. The phylogenetic tree of isolated fungus coded FL541

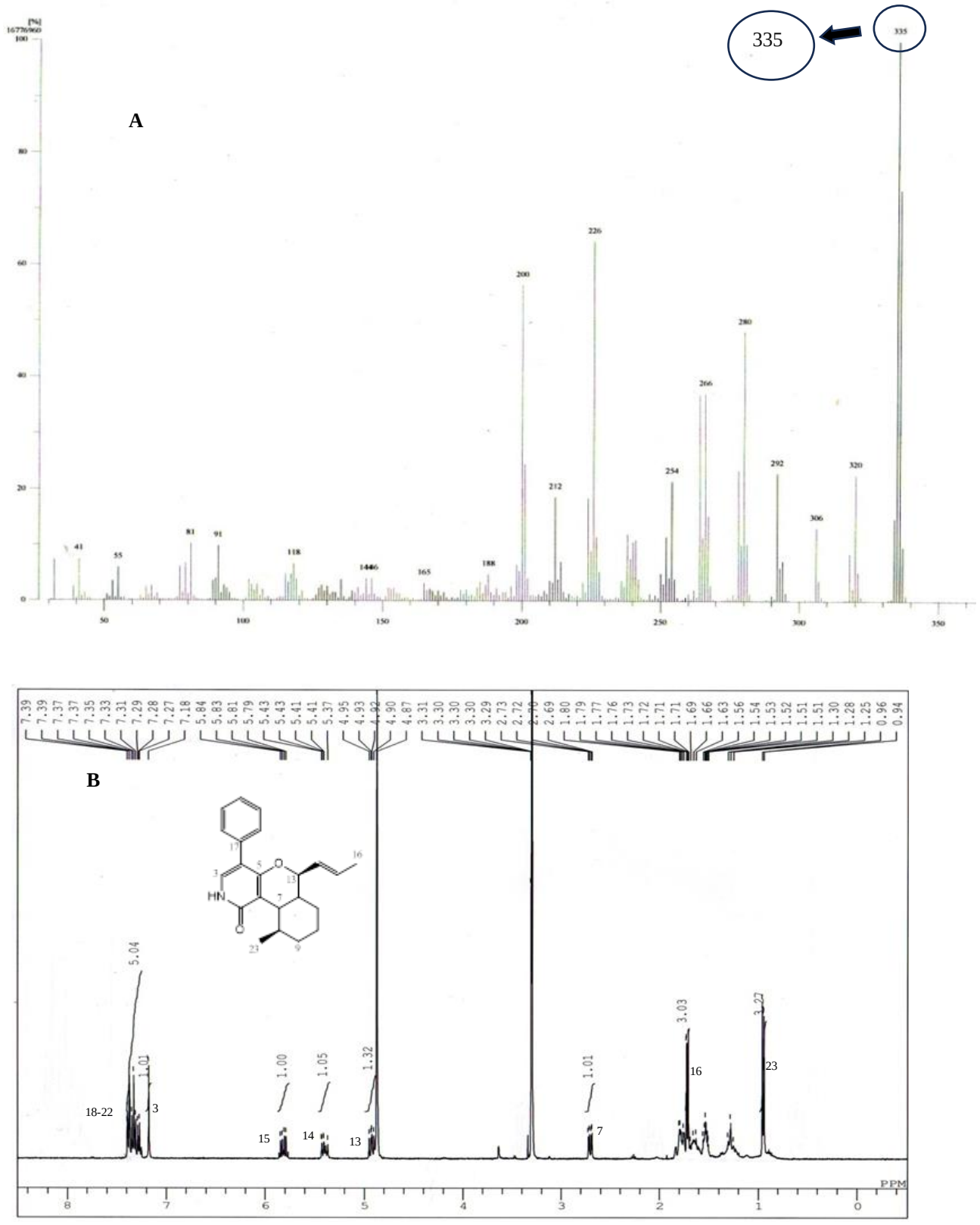

Figure 3. Mass spectra of leporin C at m/z 335 (**A**), ^{1}H NMR spectrum and the structure of leporin C (B)

Table 1. 1D (^{1}H, ^{13}C) and 2D (COSY, HMBC) NMR data of leporin C (**1**)

No.	Δ_C	type	δ_H	mult. (*J* in Hz)	COSY	HMBC
1	165.4	C				
2 (NH)		NH				
3	132.6	CH	7.18	s		1, 4, 5, 17
4	117.2	C				
5	162.2	C				
6	112.7	C				
7	38.6	CH	2.71	dd (10.9,3.6)	8, 12	1, 5, 6, 8, 9, 12, 13
8	37.4	CH	1.61	m	7, 9a, 23	
9	36.5	CH_2	1.66	m	8, 10b	
			1.23	m		
10	21.8	CH_2	1.53	m		
			1.28	m	9a, 11a	
11	27.7	CH_2	1.79	m	9a, 10b	
			1.61	m	12	
12	37.2	CH	1.76	m	11b, 13	
13	79.5	CH	4.93	dd (11.1, 8.2)	12, 14	12, 15
14	130.8	CH	5.40	dd (15.2, 8.2)	13, 15	12, 13, 16
15	132.2	CH	5.82	dq (15.2, 6.5)	14,16	13, 16
16	17.8	CH_3	1.72	dd (6.5, 1.7)	15	14, 15
17	135.7	C				
18	130.3	CH	7.38	dd (8.2, 1,4)		4
19	129.1	CH	7.34	dd (8.2, 7.2)		17
20	128.2	CH	7.27	m		18, 22
21	129.1	CH	7.34	dd (8.2, 7.2)		17
22	130.3	CH	7.38	dd (8.2, 1.4)		4
23	21.00	CH_3	0.95	d (6.8)	8	7, 8, 9

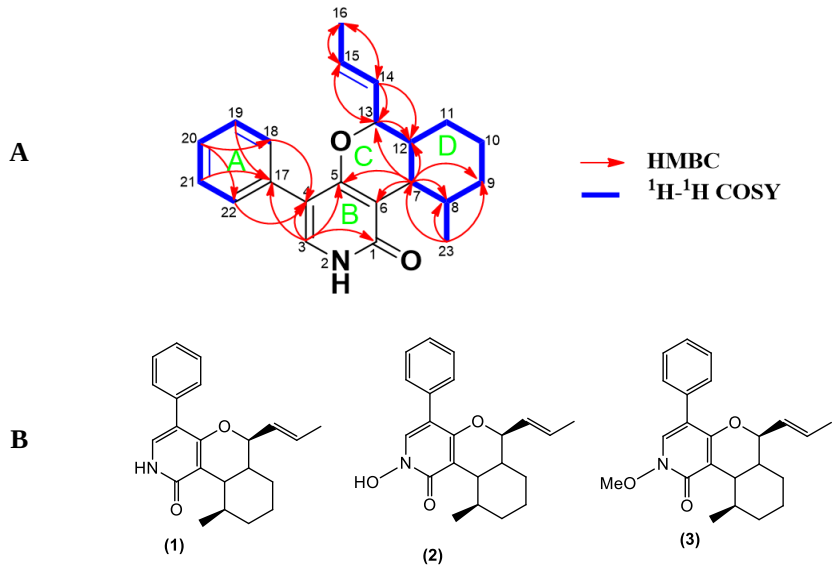

Figure 4. HMBC and COSY Correlations for leporin (**A**), structure of leporins C (**1**), B (**2**) and A (**3**) (**B**)

Biological activity of isolated compounds

Our in-house *in vitro* antimicrobial test of the isolated compounds against *S. aureus* IAM 12544T and *C. albicans* IFM 4954 showed that leporine A-C had a moderate antimicrobial activity (7-9 mm diameter of inhibition zone at 25 µg/disc) against *S. aureus* and *C. albicans.* Taking advantage of the benefits of computational studies, we further investigated the antibacterial activity of **1**-**3**.

Molecular docking studies

To determine the antimicrobial potential of the isolated compounds against FADS, we performed an in-silico test by evaluating the antimicrobial potential of the three molecules against the 2X0K protein and comparing their binding affinity to three potent FADS modulators, namely Chicago Blue 68 (**4**), Gossypol (**5**), and flunixin meglumine (**6**) (Sebastian 2018). The 2X0K protein was docked with

six ligands: leporins A-C (**1-3**), Chicago Blue Sky (**4**), Gossypol (**5**), and flunixin meglumine (**6**). Selected compound complexes were analyzed based on their Vina score, interacting amino acids, and hydrogen interactions, with the docking results presented in Table 2.

The molecular docking results showed that Chicago Sky Blue_68 or CSB_68 (**4**) had the strongest binding affinity (-10.5 kcal/mol), followed by gossypol (-9.6 kcal/mol), leporin B (-9.4 kcal/mol), leporin A (-9.1 kcal/mol), leporin C (-8.9 kJ/mol), and flunixin meglumine (-8.5 kcal/mol) (Table 2). Although two of the newly reported FADS modulators (CSB_68 and gossypol) showed slightly stronger binding affinity compared to leporins A-C (**1-3**), the isolated compounds exhibited stronger modulating activity (-8.9 to -9.6 kcal/mol) than one of the modulators, flunixin meglumine (**6**).

Moreover, Table 3 displays three different binding modes of the six ligands on the 2X0K protein. Firstly, Chicago Sky Blue 68 (**4**) interacted with amino acids in both chains A-of pocket 5 of the protein (Table 2). Additionally, three compounds (leporin A, leporin C, and flunixin meglumine) interacted with amino acids in pocket C1, chain B of the protein. Among these, leporin A and C exhibited virtually the same interacting amino acids, except for the presence of Tyr1106 in leporin A. However, both compounds only showed low similarity of interacting amino acids with flunixin meglumine (Table 2). Finally, leporin B and gossypol interacted with pocket C3 and Chain A of the protein, demonstrating more than 50% similarity of interacting amino acids (Table 2).

These results indicate that two molecules with similar structures may or may not bind to similar or different binding sites of a receptor, as seen in the case of leporin B. Despite its similar core structure to leporins A and C, leporin B did not bind to the same pocket or interact with the corresponding amino acids as leporins A and C. Instead, it bound to pocket C Chain A and interacted with various amino acids, similar to those of gossypol, which has unrelated molecular structures to leporin B (Table 2). Similarly, although to a lesser extent, flunixin meglumine (**6**) bound to pocket C1 and chain B of the receptor and interacted with Gly1022, Val1023, Phe1054, and His1057, similar to leporin A (**3**) and leporin C (**1**) (Table 2). These 3D interactions highlight the specific and strong modulating abilities of the isolated compounds with FADS (Figure 5).

We further investigated the interactions between the ligands and the receptors by focusing on the hydrogen bonds and hydrophobic interactions of the six ligands with 2X0K (Figure 6). The known FADS modulators, except for Chicago Sky Blue 68, mainly interacted with the protein target through hydrogen bonds (Table 3). In contrast, leporins A-C (**1-3**) interacted with 2X0K mainly through hydrophobic interactions (Table 3). These results suggest that the significant binding affinity of leporins A-C is largely determined by the hydrophobic interactions of the pyridone-containing molecules with the protein target rather than by hydrogen bonding.

Table 2. Docking on leporins A-C and FADS modulators against 2X0K target protein

Ligands	Vina score (Kcal/Mol)	Interacting amino acids
Leporin C (**1**)	-8.9	Pocket C1, Chain B, 1887 Å: Gly1022, Val1023, Phe1054, His1057, Pro1058, Val1059, Phe1062, Phe1094, Leu1098, Asn1125, Phe1126, Thr1127 Phe1128, Gly1129, Asn1131, Ala1132 (16).
Leporin B (**2**)	-9.4	Pocket C3: Chain A, 1203 Å: Ile21, Gly22, Val23, His28, Gly30, His31, Leu34 Val122, Gly123, Asn125, Phe126, Thr127, Leu154, Leu155, Ile162, Ser163, Ser164 Thr165, Arg168.
Leporin A (**3**)	-9.0	Pocket C1, Chain B, 1887 Å: Gly1022, Val1023, Phe1054, His1057, Pro1058, Val1059, Phe1062, Phe1094, Leu1098, Tyr1106, Asn1125, Phe1126 Thr1127, Phe1128, Gly1129, Asn1131, Ala1132 (17).
Chicago Sky Blue_68 (**4**)	-10.5	Pocket C5, Chain A and B, Cavity volume 959 Å. Chain A: Asp55 His57 Ser60 Arg65 Ala67 Pro68 Leu69 Gly70 Thr73 Ala75 Glu76 Thr190 Gly191 Pro192 Tryr212 Phe213 His214 Thr216 Val217 Leu232 Pro233 Thr234 Asp282. Chain B: Pro1192 Arg1195 Leu1232 Pro1233 Thr1234 Glu1235 Ala1236 Tyr1279 Gly1280 His1281 Asp1282.
Gossypol (**5**)	-9.6	Pocket C3: Chain A, 1203 Å: Ile21, Gly22, Val23, Phe24, His28, His31, Leu34 Phe54, His57, Pro58, Phe62, Phe94, Ser99, Asn125, Phe126, Thr127, Gly129 Asn131, Ala132, Leu154, Ser164, Thr165, Arg168 (23).
Flunixin meglumine (**6**)	-8.5	Pocket C1: Chain B, 1887 Å: Gly1022, Val1023, Phe1024, Asp1025, His1028 Gly1030, His1031, Leu1034, His1057, Gly1123, Ala1124, Asn1125, Ile1152, Asp1153, Leu1154, Leu1155, Ile1162, Ser1163, Ser1164 (19).

Table 3. Protein ligand interaction between ligands (1-6) and 2X0K protein

Ligand	Hydrogen Bonds	Hydrophobic interaction
Leporin A	Gly1129B	Val1023B, Phe1054B, Pro1058B, Phe1062B, Phe1062B, Ala1132B
Leporin B	-	Val1023B, Phe1054B, Phe1062B, Phe1062B, Ala1132B
Leporin C	-	Val1023B, Phe1054B, Phe1062B, Phe1062B, Ala1132B
Chicago Sky Blue_68	Trp4A, Tyr5A, Asp93A, Gly1200B, Lys1202B, Ser1239B, Ser1239B, Gly1240B, Gly1240B, Asp1275B, Asp1275B Asp1275B.	Tyr5A, Arg1199B, Lys1202B, Asp1275B
Gossypol	Val23A, Phe54A, Pro58A, Phe62A, Phe94A, Phe94A, Phe126A	His31A, Ser164A
Flunixin meglumine	Asn125A, Asn125A, Ser164A, Ser164A, Ser164A, Ser164A, Thr165A, Thr165A	Val23A, Leu34A

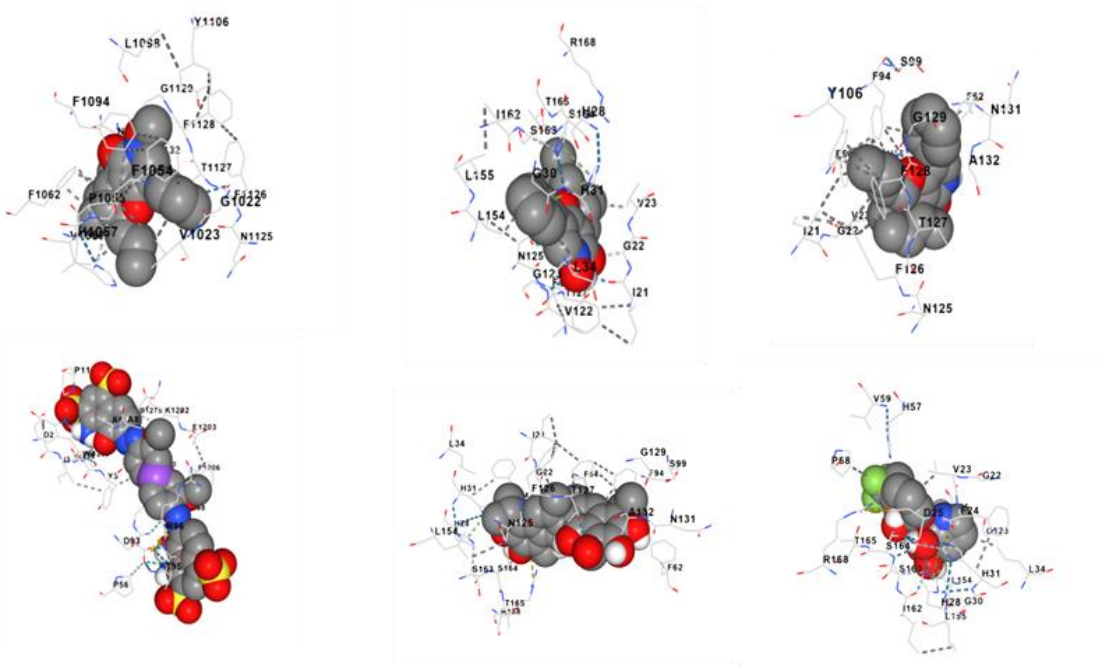

Figure 5. The 3D structure of all ligands (leporins A-C, **1**-**3**) and FADs (**4**-**6**) against the target protein

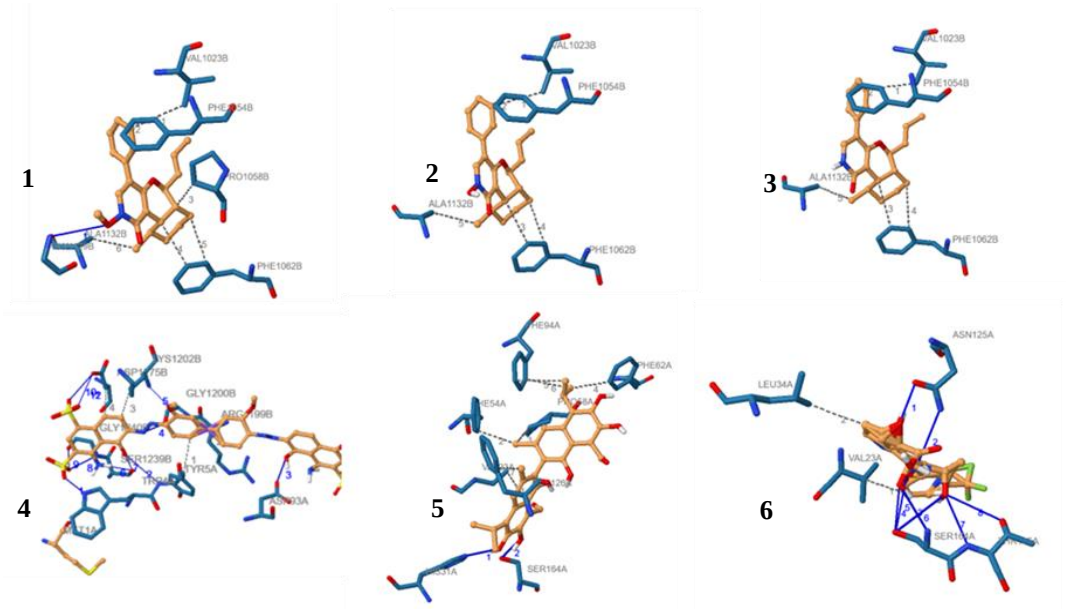

Figure 6. 3D structure of all ligands (leporins A-C, **1**-**3**) and FADS modulators (**4**-**6**) against 2X0K protein with solid lines representing hydrogen bonds and dotted brown lines representing hydrophobic interactions

Interestingly, although the contribution of hydrophobic interactions to binding affinity has often been overlooked in comparison to hydrogen bonding and electrostatic interactions in nucleic acids, increasing evidence indicates that hydrophobic interactions play a crucial role (Patil et al. 2010; Xiao et al. 2020). According to Xiao et al. (2020), hydrophobic interactions possess unique properties, such as high tunability for application interest, low effect on nucleic acid functionality, and sensitivity to external stimuli. Moreover, Feng et al. (2019) revealed the role of hydrophobic interactions in DNA in dictating biological activity, presumably due to their catalytic roles in activating DNA polymerase, implying the importance of hydrophobic interactions for biomedical applications. This appears to be the case for the binding affinity of leporins A-C towards 2X0K in the present study, although further research is needed to fully understand this claim.

Drug likeness and ADME evaluation

Finally, we evaluated the physiochemical properties of leporins A-C against the 2X0K ligand by using SwissADME on the canonical SMILES of the molecules obtained from PubChem (Table 4). The results showed that leporins A-C have high gastrointestinal absorption, moderate water solubility, and a bioavailability score of 0.55. Although the consensus log Po/w coefficient (log Po/w) of all compounds was greater than 1.2-1.8, an ideal drug-likeness for oral drugs, and leporin A and B violated one of the five Lipinski rules, all compounds were moderately lipophilic with Log P less than 5.0 and met the Lipinski rules of 5 (Lipinski 2004). Whereas all of the FADS' modulators (compounds **4-6**) had a low water solubility, except for flunixin meglumine and GI absorption. Leporins A-C, on the other hand, showed moderate water solubility and high GI absorption, indicating the potential of leporins A-C as specific modulators of FADS. Nevertheless, pkCSM data analysis showed that, despite having acceptable physicochemical profiles, leporins B and C exhibited hepatotoxicity (Table 4).

Hence, we performed a bioisosterism approach to improve both the bioactivity and ADMET profiles of the leporin structure class. One way is to applying Grimm's hydride replacement law, in which fluorine, hydroxyl, amino and methyl group interchanges (Patani and LaVoie, 1996) in, we putatively replaced a methyl group at the cyclohexyl functionality of leporin A-C with a fluorine atom as a bioisostere of the methyl group using ChemiDraw 12 to obtain leporifluorin A (**3a**), leporifluorin B (**3b**), and leporifluorin C (**3c**) or by applying a slightly modified method of the total synthesis of leporin A (Snider and Lu, 1996). Both molecular docking and ADMET analysis showed improved binding affinities, with values changing from -9.6, -9.7, and -9.8 in leporin A-C to -10.5, -10.7, and -11.1 in leporifluorin A-C (Figure 7). In addition to improving binding affinity, the substitution of a methyl group with a fluorine atom also led to improvements in the physicochemical properties of leporifluorins A-C, particularly in terms of herG I, herg II (Human ether-ago-go-related Gene (hERG), an unusual target for Protease-mediated damage (Lamothe et al. 2016), AMES or a bacterial bioassay accomplished *in vitro* to evaluate the mutagenicity of various environmental carcinogens and toxins (Vijay et al. 2018) and hepatotoxicity aspects. While leporin B and C showed herg II and hepatotoxicity (Table 4), these issues were no longer present in leporins B and C, except for herg II in leporin B (Table 5). The results suggest that although the introduction of a fluorine atom did not affect the physicochemical properties of leporin A, it significantly reduced the toxicity of leporins B and C to some extent. Additionally, the results suggest that the functional groups at the pyridone moiety dictate the cytotoxicity of leporin-typed compounds (Table 6).

To date, microbial resistance remains a serious threat to humankind, representing a major global concern (Iscla et al. 2015; Dinghra et al. 2020; Tondi 2021; Pariente et al. 2022). Although it was later questioned by de Krakter et al. (2016), O'Neil (2014) predicted that by 2050, microbial resistance would be a leading cause of death, claiming 50 million lives each year. This prediction, combined with the previous lack of new antibiotic discoveries and alarming bacterial resistance, highlights the urgent need for the discovery of novel antibiotics (Pariente 2022).

The primary challenge with current antibiotic drug development is that the majority of existing antibiotics are derivatives of known antibiotics, to which microbes can quickly develop resistance (Coates et al. 2011). Reflecting on the early period of antibiotic discovery from 1920 to 1960, when 20 novel antibiotics were discovered, the authors emphasized the necessity of discovering 20 new antibiotics and their derivatives to sustain progress for the next 50 years. However, only two novel antibiotics have been developed in the last five decades (Coates et al. 2011), indicating a significant lack of new antibiotics amidst the alarming rise of resistant pathogenic microbes.

Although leporins A-C are well-known compounds, they hold potential to be developed into new antibiotics. One reason for this is their strong binding affinity against FADS, exhibiting activity similar to that of potent FADS modulators (CSB_68 and gossypol). Furthermore, when leporins A-C were fluorinated at the secondary methyl position, their binding affinity increased. Additionally, Lao et al. (2017) reported that leporin A, isolated from a hydrothermal vent fungus *Aspergillus* sp., inhibited seven bacteria at sub-micromolar concentration, including Methicillin-resistant *Staphylococcus aureus* bacteria. *Trichoderma* fungus represents one of the common soil fungi that is mostly cultivable (Gottel et al. 2011), suggesting the possibility for developing antibiotics from the leporin-typed compounds. Importantly, the presence of 2-pyridone in many bioactive compounds, their unique properties (Forrestall et al. 2021), and their ability to restrict the degree of freedom within chemical structures as well as mimic a peptide backbone (Zhang et al. 2020) offer many benefits for drug design (Tan et al. 2019). Furthermore, leporin-containing compounds have also been reported to play crucial roles in human cell functioning (Trammell et al. 2016), and many organisms are capable of retaining, degrading, and utilizing pyridone-containing molecules (Chen et al. 2018).

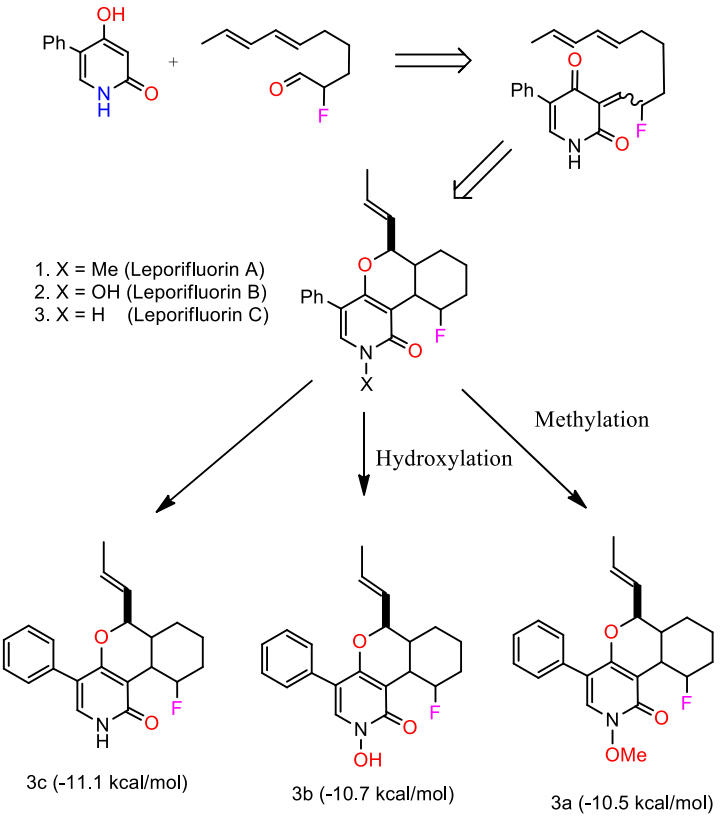

Figure 7. Replacement of a methyl group at cyclohexyl group of leporins A-C by reacting pyridone with 2-fluoro-6E,8E-decadiena instead of previously proposed 2-methyl-6E,8E-decadiena by Schnider and Lu, (1996) may result in leporifluorin C and further *N*-hydroxylation and *O*-methylation could give lepoflurin B and A respectively.

Table 4. Data of leporins A-C extracted from SwissADME

No.	Ligand	Canonical smiles	Physiochemical properties				
			Water solubility	GI Absorption	Lipinski	Bio-availability	Consensus Log P
1	Leporin A	C/C=C/[C@H](O1)C2C([C@H](C)CCC2)C3=C1C(C4=CC=CC=C4)=CN(OC)C3=O	Moderately soluble	High	Yes; 1 violation	0.55	4.27
2	Leporin B	C/C=C/[C@H](O1)C2C([C@H](C)CCC2)C3=C1C(C4=CC=CC=C4)=CN(O)C3=O	Moderately soluble	High	Yes; 1 violation	0.55	4.00
3	Leporin C	C/C=C/[C@H](O1)C2C([C@H](C)CCC2)C3=C1C(C4=CC=CC=C4)=CNC3=O	Moderately soluble	High	Yes; 0 violation	0.55	4.33
4	Chicago Sky Blue 68	COC1=C(C=CC(=C1)C2=CC(=C(C=C2)N=NC3=C(C4=C(C=C3)C(=CC(=C4N)S(=O)(=O)[O-])S(=O)(=O)[O-])O)OC)N=NC5=C(C6=C(C=C5)C(=CC(=C6N)S(=O)(=O)[O-])S(=O)(=O)[O-])O.[Na+].[Na+].[Na+].[Na+]	Poorly soluble	Low	No; 2 violation, MW>500, NorO>10	0,17	-9.06
5	Gossypol	CC1=CC2=C(C(=C(C(=C2C(C)C)O)O)C=O)C(=C1C3=C(C4=C(C=C3C)C(=C(C(=C4C=O)O)O)O)C(C)C)O)O	Poorly soluble	Low	No: 2 violation MW>500	0.55	5.50
6	Flunixin meglumine	OC(=O)c1cccnc1Nc1cccc(c1C)C(F)(F)F.CNC[C@@H]([C@H]([C@@H]([C@@H](CO)O)O)O)O	Moderately soluble	Low	Yes; 1 violation: NhorOH>5	0.55	0.91

Table 5. Data of leporins A-C extracted from pkcSM

No.	Ligand	Canonical Smiles	Physiochemical properties				
			Intestinal absorption	BBB permi-ability	Herg I/II	AMES toxicity	Hepato-toxicity
1	Leporin A	C/C=C/[C@H](O1)C2C([C@H](C)CCC2)C3=C1C(C4=CC=CC=C4)=CN(OC)C3=O	100%	High/-0.072	No/No	No	No
2	Leporin B	C/C=C/[C@H](O1)C2C([C@H](C)CCC2)C3=C1C(C4=CC=CC=C4)=CN(O)C3=O	97.40%	High/ -0.122	No/Yes	No	Yes
3	Leporin C	C/C=C/[C@H](O1)C2C([C@H](C)CCC2)C3=C1C(C4=CC=CC=C4)=CNC3=O	96.68%	High/ -0.033	No/Yes	No	Yes
4	Chicago Sky Blue 68	COC1=C(C=CC(=C1)C2=CC(=C(C=C2)N=NC3=C(C4=C(C=C3)C(=CC(=C4N)S(=O)(=O)[O-])S(=O)(=O)[O-])O)OC)N=NC5=C(C6=C(C=C5)C(=CC(=C6N)S(=O)(=O)[O-])S(=O)(=O)[O-])O.[Na+].[Na+].[Na+].[Na+]	0%	Low/ -1.976	No/No	Yes	No
5	Gossypol	CC1=CC2=C(C(=C(C(=C2C(C)C)O)O)C=O)C(=C1C3=C(C4=C(C=C3C)C(=C(C(=C4C=O)O)O)O)C(C)C)O)O	89.39%	Low	No/Yes	Yes	No
6	Flunixin meglumine	OC(=O)c1cccnc1Nc1cccc(c1C)C(F)(F)F.CNC[C@@H]([C@H]([C@@H]([C@@H](CO)O)O)O)O	4.13%	Low	No/No	No	Yes

Table 6. Binding affinities and physicochemical properties of leporifluorins A-C (**3a-6a**)

Ligand	Vina score (Kcal/mol)	Physicochemical properties									
		Water solubility	GI absorption	Lipinski	Bio-availability	Consensus Log P	Intestinal absorption	BBB Permi ability	hERG I/II inhibitors	AMES toxicity	Hepatotoxicity
Lepo fluorin A (**3a**)	–10.5	High	Yes	Yes (0V)	0.55	4.27	95.1%	0.787	No/No	No	No
Lepo fluorin B (**3b**)	–10.7	High	Yes	Yes (1V)	0.55	4.27	94.9%	0.855	No/Yes	No	No
Lepo fluorin C (**3c**)	–11.1	High	Yes	Yes (0V)	0.55	4.11	95.2%	0.787	No/No	No	No

In addition to a series of effectively developed synthetic approaches for leporin-type compounds (Snider and Lu 1994; Glöckle and Gulder 2018), the present study also demonstrates the benefits of the bioisosterism approach in enhancing the binding affinity and ADMET profiles of leporins A-C. The modification of leporins A-C by substituting a methyl group with a fluorine atom significantly improved the binding affinities and physicochemical characteristics of the modified compounds, leporifluorins **1a**-**3a**. This finding aligns with numerous recent reports highlighting the positive impact of fluorine incorporation on the bioactivity of various molecules, including but not limited to thiosemicarbazone (Patel et al. 2019) and benzazole analogs (Al-Harty et al. 2020). Moreover, the results supported the findings of Polanksi et al. (2016), who reported lower side effects and higher success rates for many fluorinated drug candidates. Nevertheless, the synthesis of such molecules remains to be proved in real experiments.

Furthermore, the advancement of bioinformatic technology has made computational studies a key strategy for discovering new antibiotics. As mentioned earlier in the introduction, in-silico studies have significantly contributed to the discovery of new antibiotic agents (Iscla et al. 2015; Khabthani et al. 2021; Stokes et al. 2020). This economical and efficient approach has contributed to the recent repurposing of known molecules or drugs for new uses. Forrestal et al. (2021), for example, reported the potential

of pyridone-containing compounds, particularly leporin A, as inhibitors of Sar-Cov-2. The present study also demonstrates that leporins A-C have the potential to be putative FADS enzyme inhibitors. Additionally, scientists from Glasco Smith designed antimicrobial compounds targeting topoisomerase II, successfully developing compounds with new targets to defeat, such as fluoroquinone, which represents a breakthrough in combating antimicrobial resistance (Bax et al. 2010).

However, it should be noted that this study was conducted using an in-silico approach, which has limitations. Therefore, further optimized *in vitro*, *in silico*, *in vivo*, or clinical and synthesis studies are required to corroborate the findings. Nevertheless, this study provides new insights of the potential of leporins A-C (**1-3**) and especially leporifluorins A-C (**1a-3a**) as FADS' modulators, and it highlights sponge symbiotic fungi as an attractive target for antimicrobial drug-lead discovery.

In conclusion, to sum up, we discovered three pyridone alkaloids, leporine A-C, from the symbiotic fungus *Trichoderma* sp. isolated from the Indonesian marine sponge *Stella clavosa*. While our in-house antimicrobial test showed that leporins A-C had moderate antimicrobial activities against *S. aureus and C. albicans*, computational studies showed that they had strong binding affinity against 2X0K, which was nearly identical to that of the newly reported FADS' modulators. Importantly, leporins A-C especially leporifluorins A-C (**1a-3a**), showed better physicochemical profiles than the majority of the reported FADS' modulators. The results suggest that leporins A-C, particularly leporins A-C (**1a-3a**), have antibacterial potential as new FADS' modulators, although further *in vivo* or *in-silico* studies as well as the synthesis of such putative modulators in real experiments are required to validate this finding. This study reveals that sponge symbiotic fungi remain an attractive source for antimicrobial lead discovery.

ACKNOWLEDGEMENTS

This research was partly supported by the Directorate of Research and Community Service of the Directorate General of Research and Development Strengthening of the Ministry of Research, Technology, and Higher Education under the 2018 Fiscal Year Research Contract Numbered: 087/SP2H/LT/DRPM/2018. We are also grateful to Prof. Michio Namikoshi and Dr. Hiroyuki Yamazaki at the Natural Product Chemistry Department, Tohoku Medical and Pharmaceutical University, for providing laboratory facilities, including spectroscopic measurements.

REFERENCES

Al-Harthy T, Zoghaib W, Abdel-Jalil R. 2020. Importance of fluorine in benzazole compounds. Molecules 25 (20): 4677. DOI: 10.3390/molecules25204677.

Bax BD, Chan PF, Eggleston DS, Fosberry A, Gentry DR, Gorrec F, Giordano I, Hann MM, Hennessy A, Hibbs M, Huang J. 2010. Type IIA topoisomerase inhibition by a new class of antibacterial agents. Nature 466 (7309): 935-940. DOI: 10.1038/nature09197.

Chen G-y, Zhong W, Zhou Z, Zhang Q. 2018. Simultaneous determination of tryptophan and its 31 catabolites in mouse tissues by polarity switching UHPLC-SRM-MS. Anal Chim Acta 1037: 200-210. DOI: 10.1016/j.aca.2018.02.026.

Coates ARM, Halls G, Hu Y. 2011. Novel classes of antibiotics or more of the same?. Br J Pharmacol 163: 184-194. DOI: 10.1111/j.1476-5381.2011.01250.x.

Daina A, Michielin O, Zoete V. 2017. SwissADME: A free web tool to evaluate pharmacokinetics, drug-likeness and medicinal chemistry friendliness of small molecules. Sci Rep 7: 42717. DOI: 10.1038/srep42717.

de Kraker ME, Stewardson AJ, Harbarth S. 2016. Will 10 million people die a year due to antimicrobial resistance by 2050? PLoS Med 13: e1002184. DOI: 10.1371/journal.pmed.1002184.

Dhingra S, Rahman NAA, Peile E, Rahman M, Sartelli M, Hassali MA, Islam T, Islam S, Haque M. 2020. Microbial resistance movements: An overview of global public health threats posed by antimicrobial resistance, and how best to counter. Front Public Health 8: 535668. DOI: 10.3389/fpubh.2020.535668.

Farhat F, Athar MT, Ahmad S, Madsen DØ, Sohail SS. 2023. Antimicrobial resistance and machine learning: Past, present, and future. Front Microbiol 14: 1179312. DOI: 10.3389/fmicb.2023.1179312.

Feng B, Sosa RP, Mårtensson AKF, Jiang K, Tong A, Dorfman KD, Takahashi M, Lincoln P, Bustamante CJ, Westerlund F, Nordén B. 2019. Hydrophobic catalysis and a potential biological role of DNA unstacking induced by environment effects. Proc Natl Acad Sci 116 (35): 17169-17174. DOI: 10.1073/pnas.1909122116.

Forrestall KL, Burley DE, Cash MK, Pottie IR, Darvesh S. 2021. 2-Pyridone natural products as inhibitors of SARS-CoV-2 main protease. Chem Biol Interact 335: 109348. DOI: 10.1016/j.cbi.2020.109348.

Glöckle A, Gulder TAM. 2018. A pericyclic reaction cascade in leporin biosynthesis. Angew Chem Intl Ed 57 (11): 2754-2756. DOI: 10.1002/anie.201800629.

Google Maps. 2023. Malalayang Beach Manado Bay. Google Maps [online] Available through: Pantai Malalayang <https://www.google.com/maps/search/Pantai+malalayang+124+derajat+49+menit+57detik/@1.460275,124.7910354,272m/data=!3m2!1e3!4b1?entry=ttu> [Accessed December 20 2023].

Gottel NR, Castro HF, Kerley M, Yang Z, Pelletier DA, Podar M, Karpinets T, Uberbacher E, Tuskan GA, Vilgalys R, Doktycz MJ, Schadt CW. 2011. Distinct microbial communities within the endosphere and rhizosphere of *Populus deltoides* roots across contrasting soil types. Appl Environ Microbiol 77: 5934-5944. DOI: 10.1128/AEM.05255-11.

Hutchings MI, Truman AW, Wilkinson B. 2019. Antibiotics: Past, present and future. Curr Opin Microbiol 51: 72-80. DOI: 10.1016/j.mib.2019.10.008.

Indraningrat AAG, Smidt H, Sipkema D. 2016. Bioprospecting sponge-associated microbes for antimicrobial compounds. Mar Drugs 14 (5): 87. DOI: 10.3390/md14050087.

Iscla I, Wray R, Blount P, et al. 2015. A new antibiotic with potent activity targets MscL. J Antibiot 68 (7): 453-462. DOI: 10.1038/ja.2015.4.

Khabthani S, Rolain J-M, Merhej V. 2021. In Silico/in vitro strategies leading to the discovery of new nonribosomal peptide and polyketide antibiotics active against human pathogens. Microorganisms 9 (11): 2297. DOI: 10.3390/microorganisms9112297.

Kobayashi H, Namikoshi M, Yoshimoto T, Yokochi T. 1996. A screening method for antimitotic and antifungal substances using conidia of *Pyricularia oryzae*. modification and application to tropical marine fungi. J Antibiot 49 (9): 873-879. DOI: 10.7164/antibiotics.49.873.

Lamothe SM, Guo J, Li W, Yang T, Zhang S. 2016. The human Ether-a-go-go-related Gene (hERG) potassium channel represents an unusual target for protease-mediated damage. J Biol Chem 291 (39): 20387-20401. DOI: 10.1074/jbc.M116.743138.

Ling LL, Schneider T, Peoples AJ, Spoering AL, Engels I, Conlon BP, Mueller A, Schäberle TF, Hughes DE, Epstein S, Jones M, Lazarides L, Steadman VA, Cohen DR, Felix CR, Fetterman KA, Millett WP, Nitti AG, Zullo AM, Chen C, Lewis K. 2015. A new antibiotic kills pathogens without detectable resistance. Nature 517 (7535): 455-459. DOI: 10.1038/nature14098.

Lipinski CA. 2004. Lead- and drug-like compounds: The rule-of-five revolution. Drug Discov Today: Technol 1 (4): 337-341. DOI: 10.1016/j.ddtec.2004.11.007.

Liu Y, Yang X, Gan J, Chen S, Xiao Z-X, Cao Y. 2022. CB-Dock2: Improved protein-ligand blind docking by integrating cavity detection, docking and homologous template fitting. Nucleic Acids Res 50 (W1): W159-W164. DOI: 10.1093/nar/gkac394.

Okamoto T, Kishimoto S, Watanabe K. 2022. Isolation of natural prodrug-like metabolite by simulating human prodrug activation in filamentous fungus. Chem Pharm Bull 70 (4): 304-308. DOI: 10.1248/cpb.c21-01099.

O'neill JI. 2014. Antimicrobial resistance: Tackling a crisis for the health and wealth of nations. Rev Antimicrob Resist 2014.

Patani GA, LaVoie EJ. 1996. Bioisosterism: A rational approach in drug design. Chem Rev 96 (8): 3147-3176. DOI: 10.1021/cr950066q.

Patel DB, Patel KD, Prajapati NP, Patel KR, Rajani DP, Rajani SD, Shah NS, Zala DD, Patel HD. 2019. Design, synthesis, and biological and in silico study of fluorine-containing quinoline hybrid thiosemicarbazide analogues. J Heterocycl Chem 56 (8): 2235-2252. DOI: 10.1002/jhet.3617.

Patil R, Das S, Stanley A, Yadav L, Sudhakar A, Varma AK. 2010. Optimized hydrophobic interactions and hydrogen bonding at the target-ligand interface leads the pathways of drug-designing. PloS One 5: e12029. DOI: 10.1371/journal.pone.0012029.

Pariente N. 2022. The antimicrobial resistance crisis needs action now. PLoS Biol 20: e3001918. DOI: 10.1371/journal.pbio.3001918.

Polanski J, Bogocz J, Tkocz A. 2016. The analysis of the market success of FDA approvals by probing top 100 bestselling drugs. J Comput Aided Mol 30: 381-389. DOI: 10.1007/s10822-016-9912-5.

Sebastián M, Anoz-Carbonell E, Gracia B, Cossio P, Aínsa JA, Lans I, Medina M. 2018. Discovery of antimicrobial compounds targeting bacterial type FAD synthetases. J Enzyme Inhib Med Chem 33: 241-254. DOI: 10.1080/14756366.2017.1411910.

Serrano A, Ferreira P, Martínez-Julvez M, Medina M. 2012. The prokaryotic FAD synthetase family: A potential drug target. Curr Pharm Des 19 (14): 2637-2648. DOI: 10.2174/1381612811319140013.

Setyowati EP, Pratiwi SUT, Hertiani T, Samara O. 2017. Bioactivity of fungi *Trichoderma reesei* associated with sponges *Stylissa flabelliformis* collected from national park West Bali, Indonesia. J Biol Sci 17 (8): 362-368. DOI: 10.3923/jbs.2017.362.368.

Schneider YK. 2021. Bacterial natural product drug discovery for new antibiotics: Strategies for tackling the problem of antibiotic resistance by efficient bioprospecting. Antibiotics 10 (7): 842. DOI: 10.3390/antibiotics10070842.

Snider BB, Lu Q. 1996. Total synthesis of (+/-)-leporin A. J Org Chem 61 (8): 2839-2844. DOI: 10.1021/jo952053i.

Shukla R, Lavore F, Maity S, et al. Teixobactin kills bacteria by a two-pronged attack on the cell envelope. Nature 608 (7922): 390-396. DOI: 10.1038/s41586-022-05019-y.

Stokes JM, Yang K, Swanson K, et al. 2020. A deep learning approach to antibiotic discovery. Cell 180 (4): 688-702. DOI: 10.1016/j.cell.2020.01.021.

Thakare R, Kesharwani P, Dasgupta A, Srinivas N, Chopra S. 2020. Antibiotics: Past, present, and future. In: Drug discovery targeting drug-resistant bacteria. Academic Press. DOI: 10.1016/B978-0-12-818480-6.00001-1.

Theuretzbacher U, Van Bambeke F, Cantón R, Giske CG, Mouton JW, Nation RL, Paul M, Turnidge JD, Kahlmeter G. 2015. Reviving old antibiotics. J Antimicrob Chemother 70 (8): 2177-2181. DOI: 10.1093/jac/dkv157.

Tan Y-N, Zeng J, Zhang S-N, Ma R-J, Pan Z-H, Tan Q-G. 2019. Pyridone alkaloids from the leaves of *Ricinus communis* and their inhibitory effect against protein tyrosine phosphatase 1B. Chem Nat Compd 55: 395-397. DOI: 10.1007/s10600-019-02702-x.

Terreni M, Taccani M, Pregnolato M. 2021. New antibiotics for multidrug-resistant bacterial strains: Latest research developments and future perspectives. Molecules 26 (9): 2671. DOI: 10.3390/molecules26092671.

Thompson JD, Higgins DG, Gibson TJ. 1994. CLUSTAL W: Improving the sensitivity of progressive multiple sequence alignment through sequence weighting, position-specific gap penalties and weight matrix choice. Nucleic Acids Res 22 (22): 4673-4680. DOI: 10.1093/nar/22.22.4673.

Trammell SAJ, Schmidt MS, Weidemann BJ, Redpath P, Jaksch F, Dellinger RW, Li Z, Abel ED, Migaud ME, Brenner C. 2016. Nicotinamide riboside is uniquely and orally bioavailable in mice and humans. Nature Comm 7: 12948. DOI: 10.1038/ncomms12948.

Tao Q, Ding C, Auckloo BN, Wu B. 2018. Bioactive metabolites from a hydrothermal vent fungus *Aspergillus* sp. YQ-13. Nat Prod Commun 13: 571-573. DOI: 10.1177/1934578X1801300514.

TePaske MR, Gloer JB, Wicklow DT, Dowd PF. 1991. Leporin A: An antiinsectan N-alkoxypyridone from the sclerotia of *Aspergillus leporis*. Tetrahedron Lett 32 (41): 5687-5690. DOI: 10.1016/S0040-4039(00)93530-5.

Tondi D. 2021. Novel Targets and mechanisms in antimicrobial drug discovery. Antibiotics 10 (2): 141. DOI: 10.3390/antibiotics10020141.

Vijay U, Gupta S, Mathur P, Suravajhala P, Bhatnagar P. 2018. Microbial mutagenicity assay: Ames test. Bio-protocol 8 (6): e2763. DOI: 10.21769/BioProtoc.2763.

Xiao F, Chen Z, Wei Z, Tian L. 2020. Hydrophobic interaction: A promising driving force for the biomedical applications of nucleic acids. Adv Sci 7 (16): 2001048. DOI: 10.1002/advs.202001048.

World Health Organization. 2021 antibacterial agents in clinical and preclinical development: An overview and analysis. WHO Genewa.

Zhang L, Lin D, Sun X, Curth U, Drosten C, Sauerhering L, Becker S, Rox K, Hilgenfeld R. 2020. Crystal structure of SARS-CoV-2 main protease provides a basis for design of improved α-ketoamide inhibiors. Science 368 (6489): 409-412. DOI: 10.1126/science.abb3405.